DATABASE ASSESSMENT OF LATERAL STRENGTH OF UNREINFORCED MASONRY WALLS ACCORDING TO EXISTING DESIGN PROVISIONS

Dinh Ngoc Hieu[1,2]*, Le Khanh Toan[1], Pham My[1], Dang Cong Thuat[1]

[1]*The University of Danang - University of Science and Technology, Vietnam*
[2]*School of Architecture, Soongsil University, South Korea*

*Corresponding author: dnhieu@dut.udn.vn

(Received: September 11, 2024; Revised: October 08, 2024; Accepted: October 15, 2024)

DOI: 10.31130/ud-jst.2024.518E

Abstract - Unreinforced masonry (URM) walls, widely used in low-rise and heritage buildings, are highly vulnerable to seismic events. Current evaluation guidelines for assessing the lateral strength of URM walls predominantly rely on empirical or semi-empirical methods derived from calibrated datasets. Consequently, a comparative analysis of the reliability of these existing provisions is essential. In this study, a comprehensive database of 146 URM walls was compiled from 26 research groups and employed to evaluate the accuracy of established guidelines, including ASCE 41-17, NZSEE, Eurocode 6, and GB50003. The comparative analysis showed that ASCE 41-17 provided the most accurate predictions with acceptable safety levels, while NZSEE produced more conservative estimates and excelled in predicting diagonal shear failure modes. Eurocode 6 showed less conservative results under high compressive stress, compared to ASCE 41-17 and NZSEE. The GB50003 model based on Mohr-Coulomb theory showed the lowest accuracy and highest variability in shear strength predictions.

Key words - Unreinforced masonry wall; In-plane lateral load-carrying capacity; Analytical model; Diagonal shear; Earthquake

1. Introduction

Unreinforced masonry (URM) walls have found widespread use globally, both in low-rise modern constructions and historical heritage buildings, owing to their cost-effectiveness, ease of assembly, and architectural aesthetics. Masonry, as a typical composite construction material, is primarily engineered to carry compression loads. However, its performance in resisting tensile and shear forces is notably deficient. Consequently, numerous studies and seismic events have exposed the inherent vulnerability of such structures to earthquakes.

For instance, during the 1994 Northridge earthquake in California, a considerable number of low-rise buildings featuring unreinforced masonry walls suffered extensive damage, including instances of collapse [1,2]. Similar observations were recorded in the aftermath of devastating earthquakes in L'Aquila, Italy, in 2009 [3], as well as in Christchurch, New Zealand, in 2010 and 2011 [4]. More recently, earthquakes with a magnitude of 5.4 Richter occurred in Gyeongju on September 12, 2016, and in Pohang on November 15, 2017, South Korea, resulting in severe damage to many low-rise residential buildings characterized by URM walls constructed before the 1980s, as depicted in Figure 1. These seismic events highlighted the susceptibility of masonry walls to shear failure, leading to significant structural damage and posing a threat to life safety.

From a structural perspective, masonry represents a non-homogeneous and orthotropic composite material, posing significant challenges in accurately predicting the mechanical properties of specific masonry units. This complexity arises due to variations in the characteristics of its constituent elements, such as the type of bricks used, the strength of mortar joints, and the quality of construction. Consequently, the behavior of masonry walls under different loading conditions is quite complicated. Figure 2 categorizes three typical in-plane failure modes of URM walls subjected to a combined action of vertical and horizontal loads: (a) rocking or toe crushing failure; (b) diagonal shear failure; and (c) sliding shear failure. Rocking or toe crushing failure (Figure 2a) is characterized by the formation of flexural cracks at the base corners along the bed joints, leading to the initial rotational movement of the masonry piers around the compressed toe. Toe crushing failure can be considered the upper limit of the rocking mode, occurring when the compressive stress in the compressed toe exceeds the masonry compressive strength. Diagonal shear failure (Figure 2b) is governed by the development of diagonal cracks that either follow the bed- and head-joints or traverse through the brick units. Finally, sliding shear failure (Figure 2c) occurs when the vertical stress is relatively low, and the quality of the mortar joints is poor, posing the sliding of a portion of the wall along the bed-joints under the action of lateral force. Usually, sliding failure of URM walls is rarely observed in the URM buildings [5].

Figure 1. *URM walls collapsed during earthquakes occurred in South Korea*

In the assessment of seismic performance of masonry structures, it is crucial to evaluate the in-plane lateral load-carrying capacity of URM walls. In current international

seismic evaluation guidelines such as ASCE 41-17 [6], NZSEE [7], Eurocode 6 [8], and GB50003 [9], different empirical formulations are specified for predicting the lateral load-carrying capacity of URM walls. ASCE 41-17 and NZSEE adopted the same approach by considering different possible failure mechanisms of URM walls subjected to in-plane lateral load, while the GB5003 prediction model is based on the Mohr-Coulomb theory. Such simplified prediction equations have primarily been established through the calibration of existing test data and simplified analytical investigations.

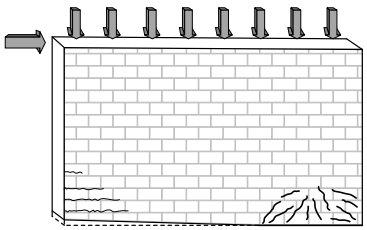

(a) Rocking / Toe crushing

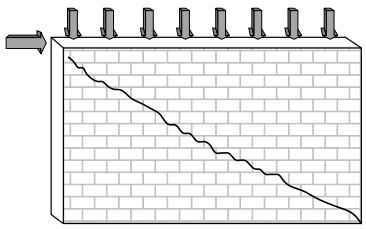

(b) Diagonal shear

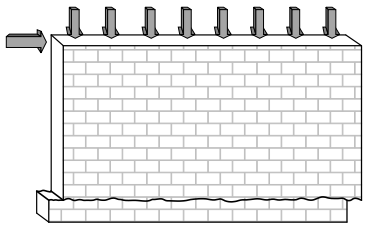

(c) Shear sliding

Figure 2. *Typical failure modes of URM walls*

Consequently, a comparative analysis of the reliability of these existing provisions is essential. In the present study, an evaluation of existing design codes and guidelines was conducted based on a large dataset from prior tests conducted on URM walls. In addition, the effects of the main influencing parameters were analyzed and discussed in detail.

2. Database evaluation and design models

2.1. Database of URM walls

The database of URM walls encompasses 146 wall specimens [10, 11]. Figure 3 presents the distribution of the specimen number according to different test parameters. The data covers a wide range of URM wall characteristics, encompassing applied compressive stress (σ_0) ranging from 0.086 to 4.0 (MPa), aspect ratios ranging from 0.21 to 2.9, wall thickness (t_w) varying from 102 to 410 (mm), and different test boundary conditions including cantilever and double fixed-end configurations.

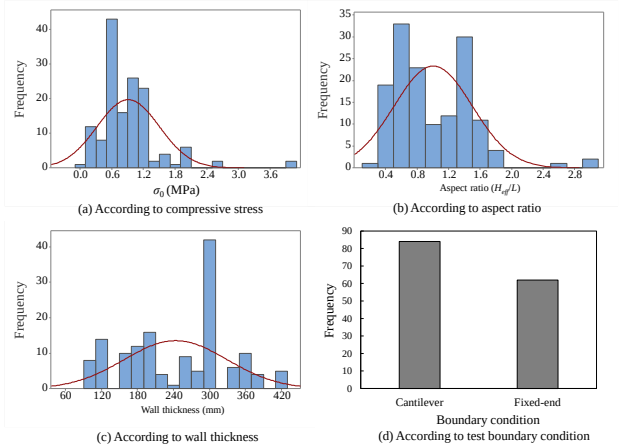

Figure 3. *Distribution of the URM walls according to test parameters in the database*

2.2. Existing design and evaluation guidelines

A comparative analysis was conducted using existing evaluation guidelines, including ASCE 41-17 [6], GB50003 [9], NZSEE [7], and Eurocode 6 [8]. The details of design equations are summarized hereafter.

- ASCE 41-17 [6]:

$$V_m = \min\,(V_{er}, V_{tc}, V_{sl}, V_{dt}) \quad (1)$$

$$V_r = 0.9(\alpha P_d + 0.5P_w)L_w / H_{eff} \quad (2)$$

$$V_{tc} = (\alpha P_d + 0.5P_w)\left(\frac{L_w}{H_{eff}}\right)\left(1-\frac{\sigma_0}{0.7f_m^{'}}\right) \quad (3)$$

$$V_{sl} = \nu_{me}A_g \quad (4)$$

$$V_{dt} = f_{dt}^{'}A_g\beta\sqrt{1+\frac{\sigma_0}{f_{dt}^{'}}} \quad (5)$$

where, P_d and P_w are the dead load and self-weight of the wall, respectively; α is the boundary condition factor (α = 0.5 for cantilever walls and α = 1.0 for both-end fixed walls); and β is a factor accounting for the non-uniform distribution of shear stress along the wall height: $\beta = 0.67$ for $L_w / H_{eff} < 0.67$, $\beta = L_w / H_{eff}$ for $0.67 \le L_w / H_{eff} \le 1.0$, and β=1.0 for $L_w / H_{eff} > 1.0$

- GB50003-2011 [9]:

$$V_m = \left(\alpha_n f_{v0} + \mu\sigma_0\right)A_g \quad (6)$$

where, α_n represents the coefficient considering the non-uniform distribution of shear stress across the cross-section; f_{v0} is the shear strength under zero compression stress; and μ is the friction coefficient.

- NZSEE [7]:

$$V_m = \min\,(V_r, V_{tc}, V_s, V_{dt}) \quad (7)$$

$$V_r = \frac{N_b}{H_w}\left[a_i - \frac{l_{er}}{3}\right] \quad (8)$$

$$V_{tc} = \frac{N_b}{H_w}\left[\frac{1}{2}L_w - \frac{1}{3}l_{etc}\right] \quad (9)$$

$$V_s = L_w t_w c + 0.8\mu_f N_t \quad (10)$$

$$V_{dt} = 0.54 L_w t_w \zeta f_{dt} \sqrt{1 + \frac{\sigma_0}{f_{dt}}} \quad (11)$$

where, N_b is the normal force acting on the cross-section of the wall base; a_i [=0.5L_w] is the distance from the compression edge of the wall to the center of gravity; l_{er} and l_{etc} are the effective lengths of the wall in rocking and toe crushing failure modes, respectively; c is the bed joint cohesion; μ_f is the coefficient of friction of the bed joint; and f_{dt} is the diagonal tension strength of the masonry unit.

- Eurocode 6 [8]:

$$V_m = \frac{f_{vk}}{\gamma_m} t_w l_c \quad (12)$$

$$l_c = 3\left(\frac{L_w}{2} - e\right) \quad (13)$$

$$e = \frac{V}{P_d} H_{eff} \quad (14)$$

where f_{vk} is the characteristics shear strength at a specified compression level σ_0; γ_m is the partial safety factor, l_c is the length of the effective uncracked section; e is the eccentricity of the vertical load (P_d) corresponding to horizontal load (V); and H_{eff} [=αH_w] is the effective height of the wall, determined by the boundary conditions of the wall (α=1.0 for cantilever walls and 0.5 for both-end fixed walls).

3. Results of comparative analysis and discussion

In the evaluation process, the input parameters required for evaluation equations in section 2.2 such as geometry properties and material properties of URM walls were directly derived from the previous publications in the database. The completed details can be found in a study by Dinh et al. [11].

Figure 4 illustrates the lateral strength ratio ($V_{test}/V_{predict}$) between the experimental results and predicted values, according to the variation of applied compressive stress acting on unreinforced masonry (URM) walls normalized by the wall compressive strength (σ_0/f'_m), and the wall aspect ratio (H_{eff}/L). The figure provides the minimum, maximum, and average values, as well as the coefficient of variation (COV) of the shear strength ratio. Additionally, the 5% fractile ($P_{0.05}$), commonly accepted as a nominal resistance value in the theory of limit states [12], was calculated to assess the safety of the design, assuming a normal distribution of the shear strength ratio. A 5% fractile value lower than 1.0 indicates an unsafe design.

Figure 4(a) shows that the ASCE 41-17 model achieves an average $V_{test}/V_{predict}$ ratio of 1.16, which closely aligns with the test results. The shear strength ratios exhibit a coefficient of variation (COV) of 0.21, and the 5% fractile value is 0.69. For cases where σ_0/f'_m > 0.15, the model's prediction of toe-crushing failure aligns with the compression failure mode of the test results. However, for σ_0/f'_m < 0.15, the ASCE model predominantly predicts shear sliding failure, which deviates from the test results. When the aspect ratio exceeds 1.0, the ASCE model predictions align well with the test results, with rocking and toe crushing as dominant failure modes.

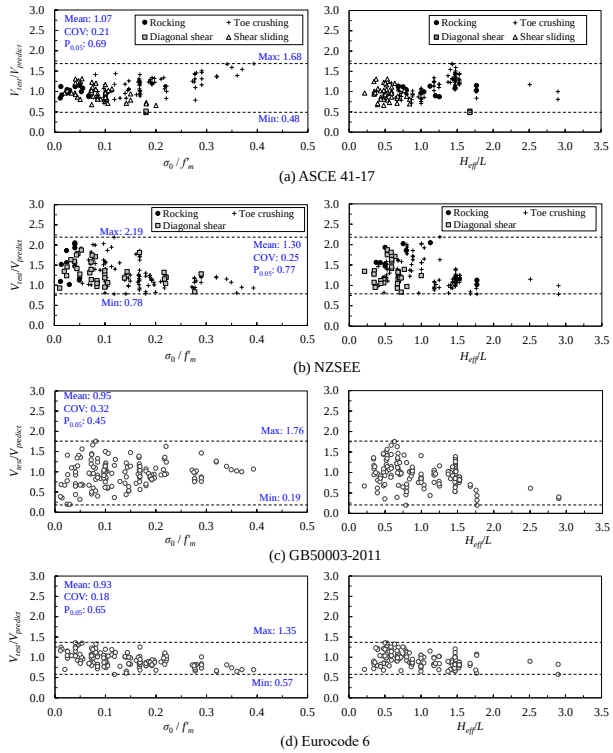

Figure 4. *Results of comparative analysis using existing design guidelines*

In Figure 4b, the NZSEE model is shown to be more conservative than the other models, with a mean strength ratio of 1.30, a COV of 0.25, and a 5% fractile value of 0.77. For walls with aspect ratios greater than 1.0, the NZSEE model predicts failure modes dominated by rocking and toe crushing, while diagonal shear failure dominates for aspect ratios below 1.0.

As depicted in Figure 4c, the GB50003-2011 model shows lower prediction accuracy compared to the previous models. Its shear strength ratio ranges from 0.19 to 1.76, with a COV of 0.32 and a notably low 5% fractile value of 0.49. The GB50003-2011 model tends to overestimate the lateral capacity of the walls when the compressive stress ratio is less than 0.5 and the aspect ratio is greater than 1.5. These discrepancies are attributed to the model's reliance on the friction failure theory, without differentiating between failure modes for unreinforced masonry (URM) walls.

In Figure 4d, the Eurocode 6 predictions show less scatter, with a COV of 0.18, but they are less conservative compared to the ASCE 41-17 and NZSEE models, particularly under high compressive stress ratios, with a 5% fractile value of 0.65 and a mean strength ratio of 0.93.

4. Parametric analysis and discussion

Figure 5 presents the results of a parametric analysis using existing design guidelines to assess the influence of key parameters on the lateral strength of unreinforced masonry (URM) walls. In Figure 5a, the effect of geometric properties is examined by varying the aspect ratio (H_w/L_w) of URM walls from 0.5 to 3.0, while keeping other parameters constant, similar to the specimens tested

by Lee et al. [13]. Figure 5b investigates the influence of the shear ratio, also varying from 0.5 to 2.0, with other parameters held constant as in the tests conducted by Petry and Beyer [14]. In Figure 5c, the primary variable is the compressive stress acting on the URM walls, ranging from 0.5 to 4.5 MPa, while other factors remain constant, following the parameters studied by Bosiljkov et al. [15].

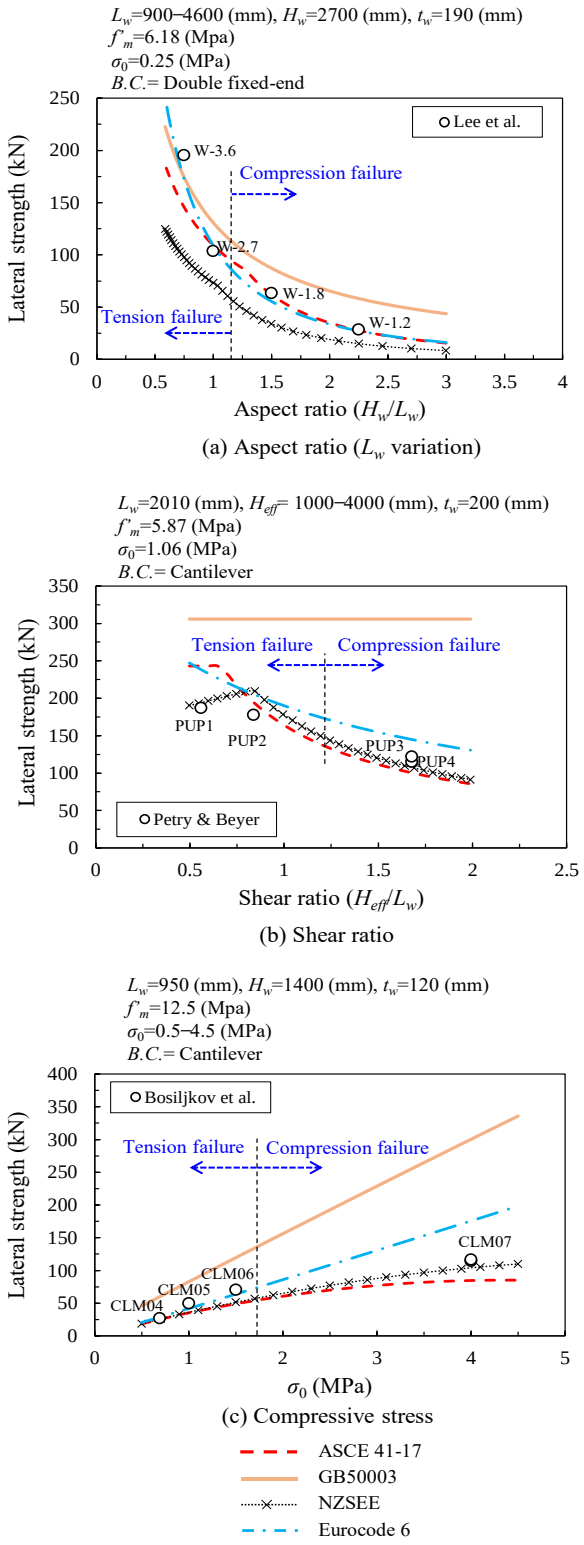

Figure 5. *Parametric analysis*

Figure 5(c) illustrates that as the compressive stress acting on URM walls increases, the predicted lateral strength also rises, aligning with the experimental findings by Bosiljkov et al. [15]. The GB50003 model tends to overestimate the lateral strength of URM walls, displaying a linear increase in strength as the applied compressive stress rises. This overestimation is attributed to the model's reliance on the Mohr-Coulomb theory, which primarily addresses friction failure and overlooks the complex failure mechanisms specific to URM walls. In contrast, the predictions made by the ASCE and NZSEE models are generally consistent and conservative when compared to the experimental results. However, the Eurocode tends to overestimate the lateral strength of URM walls, particularly under high compressive stress conditions, suggesting a limitation in accurately capturing the performance of URM walls under such loading scenarios.

5. Conclusion

In this study, a comparative analysis was conducted to assess the reliability of current design provisions for predicting the in-plane lateral load-carrying capacity of unreinforced masonry (URM) walls. The main findings from this analysis are as follows:

1. The ASCE 41-17 model provided an average $V_{test}/V_{predict}$ ratio of 1.16, which closely aligns with the test results. For low compressive stress ratio $\sigma_0/f'_m < 0.15$, the ASCE model predominantly predicts shear sliding failure, which deviates from the test results. When the aspect ratio exceeds 1.0, the ASCE model predictions align well with the test results, with rocking and toe crushing as dominant failure modes.

2. The NZSEE model provided more conservative results than the other models, with a mean strength ratio of 1.30, a COV of 0.25, and a 5% fractile value of 0.77. For walls with aspect ratios greater than 1.0, the NZSEE model predicts failure modes dominated by rocking and toe crushing, while diagonal shear failure dominates for aspect ratios below 1.0.

3. The GB50003-2011 model shows lower prediction accuracy compared to the previous models. Its shear strength ratio ranges from 0.19 to 1.76, with a COV of 0.32 and a notably low 5% fractile value of 0.49. This model tends to overestimate the lateral capacity of the walls when the compressive stress ratio is less than 0.5 and the aspect ratio is greater than 1.5.

4. Predictions from Eurocode 6 showed less scatter, with a COV of 0.18, but were less conservative than the ASCE 41-17 and NZSEE models, particularly under high compressive stress ratios. The 5% fractile value was 0.65, and the mean strength ratio was 0.93.

5. The parametric analysis showed that the ASCE 41-17 and NZSEE models consistently provided conservative predictions compared to the test results in most cases. In contrast, the Eurocode model tended to overestimate the strength of URM walls under high compressive stress. The GB50003-2011 model consistently overestimated the lateral capacity of URM walls in most scenarios.

REFERENCES

[1] J. B. Mander, M. J. Priestley, and R. Park, "Theoretical stress-strain model for confined concrete", *Journal of structural engineering*, vol. 114, no. 8, pp. 1804-1826, 1988.

[2] G. Magenes and G. M. Calvi, "In-plane seismic response of brick masonry walls", *Earthquake engineering & structural dynamics*, vol. 26, no. 11, pp. 1091-1112, 1997.

[3] A. Bosi, F. Marazzi, A. Pinto, and G. Tsionis, The L'Aquila (Italy) earthquake of 6 April 2009: report and analysis from a field mission. *EUR—Scientific and Technical Research Reports*, 2011.

[4] L. M. Moon, M. C. Griffith, D. Dizhur, J. M. Ingham, "Performance of unreinforced masonry structures in the 2010/2011 Canterbury earthquake sequence", in *Proceedings of the 15th World Conference on Earthquake Engineering (15WCEE), Lisbon, Portugal*, 2012, pp. 24-28.

[5] M. Tomaževič, "Shear resistance of masonry walls and Eurocode 6: shear versus tensile strength of masonry", *Materials and structures*, no. 42, pp. 889-907, 2009.

[6] *Seismic Evaluation and Retrofit of Existing Buildings*, ASCE 41-17, American Society of Civil Engineers, 2017.

[7] *Assessment and improvement of unreinforced masonry buildings for earthquake resistance*, NZSEE 2011, New Zealand Society for Earthquake Engineering, Wellington, New Zealand, 2011.

[8] *Design of masonry structures - Part 1-1: General rules for reinforced and unreinforced masonry structures*, Eurocode 6 (EC 6), 2005.

[9] *Code for design of masonry structures*, GB50003-2011, 2011 (in Chinese)

[10] P. Morandi, L. Albanesi, F. Graziotti, T. L. Piani, A. Penna, G. Magenes, "Development of a dataset on the in-plane experimental response of URM piers with bricks and blocks", *Construction and Building Materials*, vol. 190, pp. 593-611, 2018.

[11] N. H. Dinh, S. H. Park, S. H. Kim, K. K. Choi, and Y. J. Kim, "Analytical Model for the In-Plane Lateral Capacity of Unreinforced Masonry Walls Based on Effective Compression Zone Failure Mechanism", *Journal of Earthquake Engineering*, vol. 28, no. 16, pp. 4721–4748, 2024.

[12] *Basis of Structural Design*, EN 1990: Eurocode, European Commission, Brussels, Belgium, 2012.

[13] J. H. Lee, C. Li, S. H. Oh, W. J. Yang, and W. H. Yi, "Evaluation of rocking and toe crushing failure of unreinforced masonry walls", *Advances in Structural Engineering*, vol. 11, no. 5, pp. 475-489, 2008.

[14] S. Petry and K. Beyer, "Cyclic test data of six unreinforced masonry walls with different boundary conditions", *Earthquake Spectra*, no. 31, vol. 4, pp. 2459-2484, 2015.

[15] V. Bosiljkov, A. Page, V. Bokan-Bosiljkov, and R. Zarnic, "Performance based studies of in-plane loaded unreinforced masonry walls", *Masonry Int.*, no. 16, vol. 2, pp. 39-50, 2003.